Solid and fluid phases in smectic layers with tilted molecules

David R. Nelson and B. I. Halperin
Department of Physics, Harvard University, Cambridge, Massachusetts 02138
(Received 10 September 1979)

A recent theory of two-dimensional melting is applied to freely suspended liquid-crystal films with a tilt degree of freedom. As many as seven distinct phases are possible, including those we identify with smectic-*A*, -*B*, -*C*, and -*H* liquid crystals. Some of these phases may survive when stacked to form bulk smectics.

I. INTRODUCTION

A. Purpose

There has been considerable progress recently in understanding the mechanism of dislocation-mediated melting in two dimensions proposed by Kosterlitz and Thouless.[1,2] Although dislocations have long been suggested as a mechanism for *three*-dimensional melting,[3] only in two dimensions has substantial analytical progress been made. A study of a simplified model of interacting dislocations[4] was followed by detailed analyses[5,6] of dislocation-unbinding transitions in more realistic situations. In Ref. 5 it was found that dislocations drive a transition into a kind of liquid-crystal phase, with persistent correlations in the orientation of "bond angles." Since triangular lattices melt into a phase with persistent sixfold orientational order, this new phase might be called a "hexatic liquid crystal." A second *disclination* unbinding transition is necessary to complete the transition to an isotropic liquid.

Recent molecular-dynamics simulations by Frenkel and McTague[7] support this picture of two-dimensional melting as a two-stage process. Some evidence that dislocations were important had been obtained previously by Cotterill and Pedersen.[8] A computer simulation by Morf[9] suggests that the two-dimensional electron crystal observed by Grimes and Adams[10] melts at a temperature consistent with the dislocation-unbinding picture, provided the renormalization of the shear modulus is taken into account.

Free-standing smectic liquid-crystal films[11,12] may provide particularly interesting experimental tests of two-dimensional melting theories. One might plausibly associate a thin smectic-*B* film with a two-dimensional solid, and smectic-*A* films with two-dimensional hexatic or liquid phases. Birgeneau and Litster,[13] on the other hand, have suggested that the *bulk* smectic-*B* phases may be understood as three-dimensional analogues of the hexatic phase, with long-range orientational order and short-range translational order. If this conjecture were correct, smectic-*B* films would be examples of hexatic liquid crystals rather than two-dimensional solids. X-ray diffaction measurements by Moncton and Pindak,[14] and related work by Pershan *et al.*,[15] however, indicate that the bulk smectic-*B* phase of butoxybenzylidene-octylaniline (BBOA) possesses very long-range translational correlations. Infinite-range translational order would contradict the Birgeneau-Litster hypothesis.

Whichever interpretation is correct, it seems important to extend the theory of two-dimensional

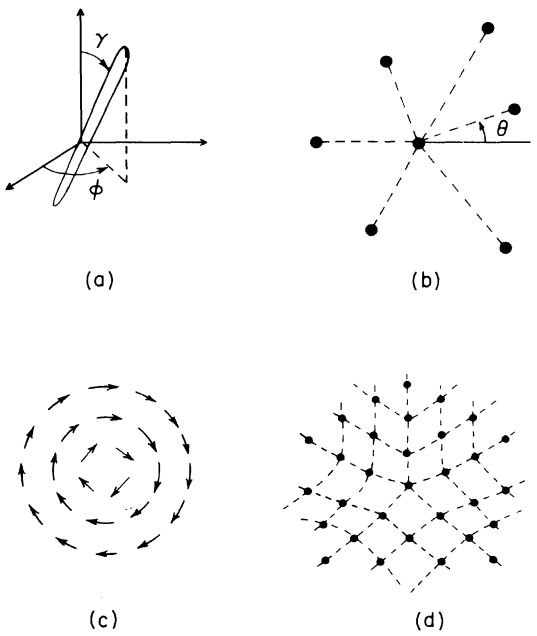

FIG. 1. Degrees of freedom and singularities necessary to describe fluid phases in smectic layers. (a) Tilted liquid-crystal molecule with polar angle γ and orientation angle ϕ. (b) "Bonds" (dashed lines) joining a central atom to its six nearest neighbors. Each such bond makes a bond angle θ with the x axis. (c) Vortex in the orientation angle field ϕ. The vectors are given by $\sin\gamma(r)[\cos\phi(r), \sin\phi(r)]$. (d) Fivefold disclination imbedded in a square lattice with bond angles shown as dashed lines.

melting to a variety of experimentally relevant situations. Here we generalize the theory to consider systems in which there is a two-dimensional vector order parameter, coupled to the order parameters that characterize melting of a triangular solid. Our work should apply in particular to thin films of materials which exhibit (in bulk) a smectic-C and/or a smectic-H phase in which there is a molecular axis tilted relative to smectic layers. Here, one must introduce an order parameter $\Phi(\vec{r}) = (\sin\gamma) \times \exp[i\phi(\vec{r})]$, which describes the projection of the tilt axis in the xy plane [see Fig. 1(a)]. Interesting effects arise from the coupling between $\Phi(\vec{r})$ and the parameters $\psi(\vec{r}) = \exp[6i\theta(\vec{r})]$ and $\rho_{\vec{G}}(\vec{r}) = \exp[i\vec{G}\cdot\vec{u}(\vec{r})]$ describing bond-angle orientations and translational order in the material [see Fig. 1(b) for a definition of the bond-orientation field].

Although we shall concentrate on applications to freely suspended films, parts of the theory may also have relevance to magnetic or orientational transitions in adsorbed films. We do not consider any electric dipolar forces associated with the molecular tilts; this is correct in a suspended film with nonchiral molecules, and may be a valid approximation in other cases if the induced dipole moment is small (cf. Refs. 11, 12, and 20).

B. Fluid phases

Couplings between orientational order and tilt degrees of freedom lead to a rich variety of possible phases and phase diagrams. Tilted and untilted versions of the hexatic and liquid phases may be understood in terms of an effective Hamiltonian functional of the bond-angle field $\theta(r)$ and tilt-phase-angle field $\phi(r)$, namely,

$$\frac{H}{k_B T} = \frac{1}{2}\int d^2r\,[\,K_6|\vec{\nabla}\theta|^2 + K_1|\vec{\nabla}\phi|^2 + 2g(\vec{\nabla}\theta)\cdot(\vec{\nabla}\phi)] - h\int d^2r\cos[6(\theta-\phi)]\ . \tag{1.1}$$

The quantity K_1 is a stiffness constant for fluctuations in the tilt orientations, while K_6 is the Frank constant for fluctuations in the bond orientation.[16] The term proportional to h occurs because both $\theta(\vec{r})$ and $\phi(\vec{r})$ feel a sixfold symmetric potential when rotated with the other field held fixed. The gradient cross-coupling, proportional to g, is generated by the renormalization group discussed in Sec. II even if it is initially absent. "Vortices" in the tilt-angle field and "disclinations" in the bond-orientation-angle fluctuations [see Figs. 1(c) and 1(d)] will also be taken into account. These excitations renormalize the elastic constants at large distances, and can also drive phase transitions by unbinding from a state containing bound pairs only. The "bare" constants in Eq. (1.1) will themselves have an analytic dependence on temperature due to the effects of fluctuations on the atomic length scale.

The constant K_6 in Eq. (1.11) is related to the Frank constant K_A used in previous papers,[5] by $K_6 = K_A/k_B T$. The subscripts 6 and 1, which we use in the present paper to indicate quantities referring to the angles θ and ϕ, respectively, were chosen because the bond orientation θ is defined modulo $\frac{2}{6}\pi$, while the tilt orientation ϕ is defined on the entire range from 0 to 2π.

A variety of possible phases follow from this model, which may be distinguished by the large-distance behavior of the correlation functions

$$C_6(\vec{r}) \equiv \langle \exp\{6i[\theta(\vec{r})-\theta(\vec{0})]\}\rangle\ , \tag{1.2a}$$

$$C_1(\vec{r}) \equiv \langle \exp\{i[\phi(\vec{r})-\phi(\vec{0})]\}\rangle\ . \tag{1.2b}$$

We summarize here the results of our analysis, whose details are given in Secs. II and III below. One possible phase diagram is shown in Fig. 2, as a function of the inverse "bare" Frank constants K_1^{-1} and K_6^{-1}, with g and h small and fixed. The quantities K_1^{-1} and K_6^{-1} should both be monotonically increasing functions of temperature, so that a given material will trace a path from lower left to upper right in the figure, as temperature is increased. The solid phases shown in this diagram, in which $K_6 = \infty$, will be discussed later.

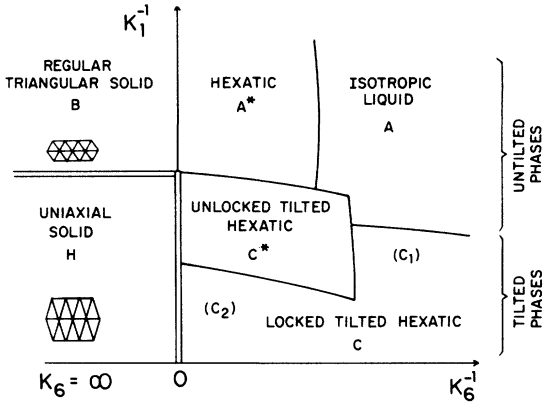

FIG. 2. Phase diagram for smectic liquid-crystal layers, as a function of the inverse temperature-dependent Frank coefficients $K_1^{-1}(T)$ and $K_6^{-1}(T)$. Both solid and fluid phases are shown, and these can be either tilted or untilted. The Frank constant K is infinite in the solid phases. Experiments with varying temperature might trace a path from the lower-left to the upper-right portion of the figure, with increasing temperatures.

Four *fluid* phases are indicated in the diagram, labeled A, A^*, C, and C^*. Phase A^* is identical to the hexatic phase of Ref. 5, with algebraic decay of $C_6(\vec{r})$ and exponential decay of $C_1(\vec{r})$,

$$C_6(\vec{r}) \simeq r^{-\eta_6(T)} , \quad C_1(\vec{r}) \simeq e^{-r/\xi_1(T)} . \tag{1.3}$$

[We shall use the term "quasi-long-range order" for correlations such as $C_6(\vec{r})$ in Eq. (1.3) which decay to zero as power laws.]

Phase A, in Fig. 2, is an isotropic liquid phase, where both $C_1(\vec{r})$ and $C_6(\vec{r})$ decay exponentially at large r. The remaining fluid phases, C and C^*, have quasi-long-range order for both tilt and bond orientations; i.e., for large r we have

$$C_6(\vec{r}) \simeq r^{-\eta_6(T)} , \tag{1.4}$$

$$C_1(\vec{r}) \simeq r^{-\eta_1(T)} . \tag{1.5}$$

Phase C is a "locked" tilted hexatic phase in which long-wave-length fluctuations in ϕ are tied to fluctuations in θ. The phase is characterized by a single renormalized (i.e., macroscopic) Frank constant K_+^R which describes the increase in energy caused by equal gradients in θ and ϕ. (Roughly one has $K_+^R \simeq K_1 + K_6 + 2g$). In this phase, the exponents η_1 and η_6 are related by

$$\eta_6 = 36\eta_1 = \frac{18}{\pi K_+^R} . \tag{1.6}$$

Phase C^* is an "unlocked" tilted hexatic phase, in which long-wavelength fluctuations in ϕ and θ are independent. This phase has three renormalized Frank constants, K_1^R, K_6^R, and g_R, corresponding to the constants in Eq. (1.1), and there is no simple relation between η_1 and η_6

$$\eta_6 = \frac{18K_1^R}{\pi(K_6^R K_1^R - g_R^2)} , \tag{1.7a}$$

$$\eta_1 = \frac{K_6^R}{2\pi(K_6^R K_1^R - g_R^2)} . \tag{1.7b}$$

Further insight into the difference between the phases C and C^* may be obtained by examining the correlation function

$$C_\Delta(\vec{r}) \equiv \langle \Delta(\vec{r})\Delta^*(\vec{0}) \rangle , \tag{1.8}$$

where $\Delta(\vec{r})$ is a variable which measures the relative orientation of the bond and tilt axes,

$$\Delta(\vec{r}) = \exp\{6i[\theta(\vec{r}) - \phi(\vec{r})]\} . \tag{1.9}$$

In the unlocked state C^*, we find the large-distance behavior

$$C_\Delta(\vec{r}) \sim (\text{const}) + r^{-\eta_\Delta} , \tag{1.10}$$

with

$$\eta_\Delta = \frac{18(K_6^R + K_1^R + 2g_R)}{\pi(K_6^R K_1^R - g_R^2)} . \tag{1.11}$$

In phase C, the locked tilted state, the correlation function $C_\Delta(\vec{r})$ tends *exponentially* towards a constant value at large r.

The unlocked phase C^* is found to be present in the phase diagram when the bare coupling constant h is small, but the state may *not* exist when h is large. Some necessary conditions for stability of the C^* phase are

$$\eta_\Delta > 4 , \tag{1.12}$$

$$K_1^R > 2/\pi , \tag{1.13}$$

$$K_6^R > 72/\pi . \tag{1.14}$$

It should be noted that quasi-long-range order in tilt orientation always induces algebraically decaying correlations of bond orientation. Thus, phases with short-range bond order but quasi-long-range tilt order are impossible. We expect that short-range bond orientational order will also be incompatible with long-range tilt-angle order in *bulk* smectic liquid crystals.

In the right-hand portion of the C phase, labeled C_1 in Fig. 2, one is in a region where there would be no bond order if the molecules were not tilted. The correlation function $C_6(\vec{r})$ has algebraic decay at long distances only because of the coupling h between tilt and bond angles, and the amplitude of the correlations should be proportional to h^2. In the left-hand portion of the C phase (labeled C_2), the bond angles would tend to order, (forming a hexatic phase) even in the absence of tilt. The amplitude of $C_6(\vec{r})$ will be independent of h in this region, and hence much larger than in the region C_1. Since there is no change in symmetry, there is no necessity for a sharp phase transition between the regions C_1 and C_2. However, there may be a first-order transition in some cases.[17,18]

C. Solid phases

In addition to the fluid phases described above, there are two solid phases (B and H) indicated in Fig. 2. These phases have true long-range order in the bond orientation,[19]

$$\langle e^{6i\theta} \rangle = (\text{const}) e^{6i\theta_0} \neq 0 , \tag{1.15}$$

where θ_0 is the orientation of the crystal axis in the xy plane. The Frank constant K_6 entering Eq. (1.1) should be considered infinite in the solid phases; however, we must now take into account coupling of the tilt orientation to the strain field of the crystal. Possible solid phases may then be understood in

terms of the effective Hamiltonian

$$\frac{H}{k_B T} = \frac{1}{2}\int d^2r\,[2\mu u_{ij}^2 + \lambda u_{kk}^2 + 2w(u_{ij} - \tfrac{1}{2}\delta_{ij}u_{kk})s_i s_j] - h\int d^2r \cos[6(\phi(r) - \theta_0)] + \tfrac{1}{2}K_1\int d^2r\,(\vec{\nabla}\phi)^2 \ , \quad (1.16)$$

where the strain tensor $u_{ij}(\vec{r})$ is the symmetric derivative of the displacement field $\vec{u}(\vec{r})$

$$u_{ij} = \frac{1}{2}\left(\frac{\partial u_i}{\partial x_j} + \frac{\partial u_j}{\partial x_i}\right) \ , \quad (1.17)$$

μ and λ are the (bare) Lamé elastic constants, and

$$\vec{s} = \begin{pmatrix}\cos(\phi - \theta_0)\\ \sin(\phi - \theta_0)\end{pmatrix} \ . \quad (1.18)$$

If the coupling proportional to w in Eq. (1.16) were neglected, one could apply the analysis of José *et al.*[20] to the tilt degrees of freedom and find three solid phases: (i) a regular triangular solid with short-range order in tilt angles; (ii) a regular triangular solid with quasi-long-range tilt-angle order; and (iii) an anisotropic solid with genuine long-range order in $\phi(\vec{r})$, i.e.,

$$\langle e^{i\phi(\vec{r})}\rangle \neq 0 \ . \quad (1.19)$$

We find, however, that the anharmonic coupling between phonons and $\vec{s}$ destabilizes the intermediate phase (ii) above. Presumably, this instability leads to a tilted anisotropic solid identical to (iii). One would then expect the line of phase transitions directly from a regular triangular untilted solid (labeled B) to an anisotropic solid with tilt (labeled H), as shown in Fig. 2.

D. Discussion

Phase boundaries shown as light solid lines in Fig. 2 are "Kosterlitz-Thouless"-type phase transitions, with unobservable essential singularities in the specific heat, but with jumps in appropriate stiffness constants. The double lines represent transitions whose character has not been analyzed.

On the line connecting locked tilted hexatic phase C to the isotropic liquid (this may be considered as a line of smectic-A to smectic-C phase transitions), one has $\eta_1 = \frac{1}{4}$, as discussed by Nelson and Kosterlitz[21] and Pelcovits and Halperin.[22] It follows from Eq. (1.6) that $\eta_6 = 9$ on this line. On the line joining the hexatic and isotropic liquid phases, one finds $\eta_6 = \frac{1}{4}$, as discussed in Ref. 5. In contrast, η_1, η_6, and η_Δ are nonuniversal and subject to only mild restrictions on the boundaries of the unlocked tilted hexatic phase (see Sec. II B).

The complicated array of phases and phase transitions described above is interesting for a number of reasons. First, the phases with quasi-long-range or long-range order in the tilt angle should be optically active and accessible to light-scattering studies. Orientational order in the hexagonal bond fields, which cannot be directly probed by optical methods, can thus be studied indirectly through its coupling to the tilt angle. Second, one might hope our results have some relevance to *bulk* smectic liquids crystals. The labels A and C in Fig. 2 were chosen because the corresponding phases have the properties of an isolated layer of the bulk phases known as smectic A and smectic C, respectively. Similarly, phases B and H correspond to the most commonly accepted description of the bulk smectic-B and -H phases, in which the smectic layers are believed to be two-dimensional solids. A stack of two-dimensional solids with any finite coupling between the layers would be expected to form (in thermal equilibrium) a three-dimensional solid, with conventional long-range translational order in all directions. Recent x-ray measurements on the smectic-B phase of the compound BBOA support this description.[14,15]

As pointed out by Birgeneau and Litster,[13] a stack of weakly coupled hexatic layers (the A^* phase) would form a bulk liquid-crystal phase, with short-range translational order parallel to the layers, but long-range order in the bond-angle field, $\langle\psi\rangle \neq 0$. Experimental identification of such a phase has not been reported, however.

The unlocked tilted hexatic C^* should not have any analog in three dimensions. If the tilt orientation has true long-range order, it will always be locked to θ.

In Sec. II, below, we shall discuss the fluid phases A, A^*, C, and C^*, in the limits of both weak and strong coupling between bond and tilt orientations. The effect of tilt on two-dimensional solids is described in Sec. III. Derivations of renormalization-group recursion relations are contained in an Appendix A, and the behavior of a correlation function is worked out in Appendix B.

II. HEXATIC AND LIQUID PHASES WITH TILT

A. Weak-coupling Hamiltonian

As discussed in the Introduction, a reduced effective Hamiltonian describing hexatic and liquid phases with tilt is[16]

$$-\bar{H} \equiv \frac{H}{k_B T} = \frac{1}{2}\int d^2r\,[K_6(\vec{\nabla}\theta)^2 + K_1(\vec{\nabla}\phi)^2 + 2g(\vec{\nabla}\theta)\cdot(\vec{\nabla}\phi)] - h\int d^2r \cos[p(\theta - \phi)] \ , \quad (2.1)$$

where we have generalized Eq. (1.1) to allow for a $p$fold symmetric coupling between $\theta(\vec{r})$ and $\phi(\vec{r})$. The probability of a given configuration of bond and tilt orientation angles is proportional to $\exp \overline{H}$, and the partition function corresponding to Eq. (2.1) is given by a functional integral over θ and ϕ,

$$Z = \int D\theta \int D\phi \exp \overline{H} \ . \tag{2.2}$$

Although we shall focus primarily on the case $p=6$, other values of p are possible. Square lattices should melt into "tetratic" liquid-crystal phases,[5] in which $p=4$ would be appropriate. One can use the model with $p=3$ to describe symmetric molecules tilted completely into the plane of the film [$\gamma = \frac{1}{2}\pi$ in Fig. 1(a)], provided one redefines θ and ϕ to be twice the angle between the x axis and the bond or molecular orientation. (If θ and ϕ are not redefined in this way, one has $p=6$, but then half-integer vortices in the θ field must be considered.[23]) Here we consider only integral vortices in ϕ, but allow for a $p$fold symmetric θ field. Our analysis can easily be extended to completely general situations.

In the limit of infinite K_6, the θ field is locked to some constant value, and Eq. (2.1) reduces to a model where rotational invariance in ϕ is broken by a $p$fold symmetric "crystal field." With vortices taken into account, this is the "cos$p\phi$" model of xy magnetism studied extensively by José *et al.*[20] Our conclusions should reduce to the known results for this system in the limit $K_6 \to \infty$ (see below). In the limit $K_1 \to \infty$, the ϕ field is locked, and one is left with a $p$fold-symmetric field θ subject to a cos$p\theta$ perturbation. Since this situation is like an xy model in a magnetic field, one expects no phase transition with varying K_6 in this limit. Note that one must have

$$g^2 < K_6 K_1 \tag{2.3}$$

in Eq. (2.1) for stability.

Strictly speaking, *all* terms in Eq. (2.1) should be periodic under the transformation

$$\theta(\vec{r}) \to \theta(\vec{r}) + \frac{2\pi}{p} m(\vec{r}) \ , \quad m(\vec{r}) = 0, \pm 1, \ldots \ , \tag{2.4a}$$

$$\phi(\vec{r}) \to \phi(\vec{r}) + 2\pi n(\vec{r}) \ , \quad n(\vec{r}) = 0, \pm 1, \ldots \ , \tag{2.4b}$$

and the functional integrals in Eq. (2.2) need only be carried out over the range

$$-\frac{\pi}{p} \leq \theta(\vec{r}) \leq \frac{\pi}{p} \ , \tag{2.5a}$$

$$-\pi \leq \phi(\vec{r}) \leq \pi \ . \tag{2.5b}$$

This periodicity reflects the invariance of the systems to discrete local rotations of θ and ϕ, with angles in other regions of space held fixed. In practice, however, studies of the two-dimensional xy model[20,24] suggest that one can integrate freely provided the disclination and vortex singularities allowed by Eq. (2.4) are taken into account explicitly.

These textural singularities can be included in Eq. (2.1) for small h as follows. At every point in space, the exponentiated periodic potential can be expanded in a Fourier series,

$$\exp\left(h \cos\{p[\theta(\vec{r}) - \phi(\vec{r})]\}\right) = \sum_{s(\vec{r})=-\infty}^{+\infty} A_s(h) \exp\{ips(\vec{r})[\theta(\vec{r}) - \phi(\vec{r})]\} \ . \tag{2.6}$$

It can readily be shown that, for small h,

$$A_s(h) \simeq (\tfrac{1}{2}h)^{s^2}, \quad s = 0, \pm 1 \tag{2.7}$$

and $A_s(h)$ is negligible for large s. More generally, one can take

$$A_s(h) \equiv A_0 \exp[(\ln y_h) s^2] \ , \tag{2.8}$$

where Eq. (2.7) is recovered if we take

$$y_h = \tfrac{1}{2}h, \quad A_0 = 1 \ . \tag{2.9}$$

Inserting the decomposition (2.6) into Eq. (2.2), one finds that the partition sum acquires a sum over an integer-valued field $\{s(\vec{r})\}$,

$$Z = \sum_{\{s(\vec{r})\}} \int D\theta \int D\phi \exp[\overline{H}(\{\theta\}, \{\phi\}, \{s\})] \ , \tag{2.10}$$

with

$$\begin{aligned} \overline{H} = -\tfrac{1}{2} \int d^2r \, [K_6(\vec{\nabla}\theta)^2 + K_1(\vec{\nabla}\phi)^2 \\ + 2g(\vec{\nabla}\theta)\cdot(\vec{\nabla}\phi)] \\ + ip \int d^2r \, s(\vec{r})[\theta(\vec{r}) - \phi(\vec{r})] \\ + (\ln y_h) \int d^2r \, s^2(\vec{r}) \ . \end{aligned} \tag{2.11}$$

As h tends to zero, $\ln y_h$ becomes large and negative, and excitations with $s(r)$ nonzero at some point become very unlikely. "Vortices" and "disclinations" can then be defined as solutions of

$$K_6 \nabla^2\theta + g\nabla^2\phi = 0 \ , \tag{2.12a}$$

$$K_1 \nabla^2\phi + g\nabla^2\theta = 0 \ , \tag{2.12b}$$

subject to conditions on contour integrals taken around isolated points $\vec{r}$,

$$\oint \vec{\nabla}\theta \cdot d\vec{l} = \frac{2\pi}{p} m(\vec{r}) \ , \quad m(\vec{r}) = 0, \pm 1, \ldots \ , \tag{2.13a}$$

$$\oint \vec{\nabla}\phi \cdot d\vec{l} = 2\pi n(\vec{r}) \ , \quad n(\vec{r}) = 0, \pm 1, \ldots \ . \tag{2.13b}$$

Expanding $\theta(r)$ and $\phi(r)$ about disclination and vortex complexions described by $\{m(\vec{r})\}$ and $\{n(\vec{r})\}$ amounts to making the substitutions

$$\theta(\vec{r}) = \delta\theta(\vec{r}) + \frac{1}{6}\sum_{\vec{r}'\neq\vec{r}} m(\vec{r}')\tilde{G}(\vec{r},\vec{r}') \ , \quad (2.14a)$$

$$\phi(\vec{r}) = \delta\phi(\vec{r}) + \sum_{\vec{r}'\neq\vec{r}} n(\vec{r}')\tilde{G}(\vec{r},\vec{r}') \quad (2.14b)$$

and then integrating freely over $\delta\phi$ and $\delta\phi$. The summations in Eq. (2.14) cover a lattice of possible sites for disclinations and vortices. This same lattice can be used to provide an ultraviolet cutoff of order the inverse core diameter a^{-1} for the functional integrations in Eq. (2.2). It has no further physical significance. For large separations $(\vec{r}-\vec{r}')$ and far from boundaries, the Green function $\tilde{G}(\vec{r},\vec{r}')$ is

$$\tilde{G}(\vec{r},\vec{r}') \simeq \tan^{-1}\left[\frac{y-y'}{x-x'}\right] \ , \quad (2.15)$$

where $\vec{r}=(x,y)$ and $\vec{r}'=(x',y')$.

Upon making the replacements (2.14) in Eq. (2.11), one easily carries out the functional integrations over $\delta\theta$ and $\delta\phi$ to find

$$Z = (\text{const}) \sum_{\{s(\vec{r})\}}{}' \sum_{\{m(r)\}}{}' \sum_{\{n(r)\}}{}' \exp[\bar{H}(\{s\},\{m\},\{n\})] \ , \quad (2.16)$$

where $\bar{H}$ is expressible in terms of three coupled Coulomb-gas Hamiltonians

$$\bar{H} = \bar{H}_c(K_h,y_h,\{s\}) + \bar{H}_c\left(\frac{K_6}{p^2},y_6,\{m\}\right) + \bar{H}_c(K_1,y_1,\{n\}) + i\sum_{\vec{r}\neq\vec{r}'} s(\vec{r})m(\vec{r}')\tan^{-1}\left[\frac{y-y'}{x-x'}\right]$$
$$- ip\sum_{\vec{r}\neq\vec{r}'} s(\vec{r})n(\vec{r}')\tan^{-1}\left[\frac{y-y'}{x-x'}\right] + \frac{2\pi g}{p}\sum_{r\neq r'} m(\vec{r})n(\vec{r}')\ln\left[\frac{|\vec{r}-\vec{r}'|}{a}\right] \ . \quad (2.17)$$

The Hamiltonian $\bar{H}_c$ is the usual[24] scalar Coulomb gas,

$$\bar{H}_c(K,y,\{m\}) \equiv \pi K\sum_{\vec{r}\neq\vec{r}'} m(\vec{r})m(\vec{r}')\ln\left[\frac{|\vec{r}-\vec{r}'|}{a}\right] + \ln y\sum_r m^2(r) \ . \quad (2.18)$$

The disclination and vortex fugacities y_6 and y_1 are

$$y_6 = \exp(-CK_6/p^2), \quad y_1 = \exp(-C'K_1) \ , \quad (2.19)$$

where C and C' are cutoff-dependent constants. The strength K_h of the logarithmic interaction between the $\{s(\vec{r})\}$ generated by integrating over θ and ϕ is

$$K_h = \frac{p^2(K_6+K_1+2g)}{4\pi^2(K_6K_1-g^2)} \ , \quad (2.20)$$

and the corresponding fugacity is given by Eq. (2.9). The primes on the summations over the three integer fields in Eq. (2.16) mean they are subject to the constraints

$$\sum_{\vec{r}} s(\vec{r}) = \sum_{\vec{r}} m(\vec{r}) = \sum_{\vec{r}} m(\vec{r}) = 0 \ . \quad (2.21)$$

In deriving Eq. (2.17), it is helpful to use the identity

$$[\vec{\nabla}\tilde{G}(\vec{r},\vec{r}')]^2 = [\vec{\nabla}G(\vec{r},\vec{r}')]^2 \ , \quad (2.22)$$

where $G(r,r')$ is the harmonic conjugate of $\tilde{G}(r,r')$ and satisfies

$$\nabla^2 G(\vec{r},\vec{r}') = 2\pi\delta(\vec{r}-\vec{r}') \ . \quad (2.23)$$

Far from boundaries and for large $(\vec{r}-\vec{r}')$, one has

$$G(\vec{r},\vec{r}') \simeq \ln(|\vec{r}-\vec{r}'|/a) + 2\pi C \ . \quad (2.24)$$

If we take the limit $K_6 \to \infty$ or $K_1 \to \infty$ in Eq. (2.17), so that either disclination or vortex pair excitations are unlikely, then one can safely set either all $m(\vec{r})$ or all $n(\vec{r})$ to zero. In this case, the Hamiltonian (2.17) reduces to an expression derived by Kadanoff[25] for the xy models with $\cos p\theta$ perturbations using a different method.

B. Weak-coupling phase diagram

The statistical mechanics of the interacting disclinations, vortices, and "periodic excitations" $\{s(\vec{r})\}$ described by Eq. (2.17) can be studied by a triple expansion in the fugacities y_6, y_1, and y_h. Experience with the xy model[20,24] suggests that such perturbation series will either diverge, or instead give only small corrections to the behavior obtained in the absence of disclinations, vortices, or periodic couplings. The corresponding fugacities will be "relevant" or "irrelevant" variables depending on the magnitudes of K_6, K_1, and g. If it is known that vortices and the y_h

coupling can be neglected, for example, then the crucial integral which determines the importance of disclinations is

$$2\pi \int_a^\infty r^3 \langle m(\vec{r}) m(\vec{0}) \rangle \, dr \simeq -4\pi y_6^2 \int_a^\infty dr \, r^{3-2\pi K_6/p^2} \quad . \tag{2.25}$$

The corresponding renormalization-group eigenvalue for the fugacity y_6 is

$$\lambda_6 = 2 - \pi K_6/p^2 \quad , \tag{2.26}$$

where the sign of λ_6 determines the convergence of the integral in Eq. (2.25). Similar considerations lead to the eigenvalues for y_1 and y_h, namely,

$$\lambda_1 = 2 - \pi K_1 \quad , \tag{2.27}$$

$$\lambda_h = 2 - \pi K_h \quad , \tag{2.28}$$

where K_h is given by Eq. (2.20). [More precisely, for large length scales we must use the renormalized elastic constants in Eqs. (2.26)–(2.28).]

A more detailed derivation of these results, together with more complete renormalization-group recursion relations (see Appendix A), will be given in Sec. II C. A crude, but qualitatively correct phase diagram, however, follows from considering regions with different stability properities determined by the eigenvalues quoted above. For example, for $p=6$, there is a region in the space of K_1^{-1}, K_6^{-1}, and g in which all three fugacity eigenvalues are negative. In Fig. 3, which illustrates the plane $g=0$, the region is the trapezoid *ABCD*. Although the figure is drawn for $g=0$, it is qualitatively similar for finite g. The trapezoid becomes a triangle for $p \lesssim 4$, and vanishes altogether for slightly smaller p's.

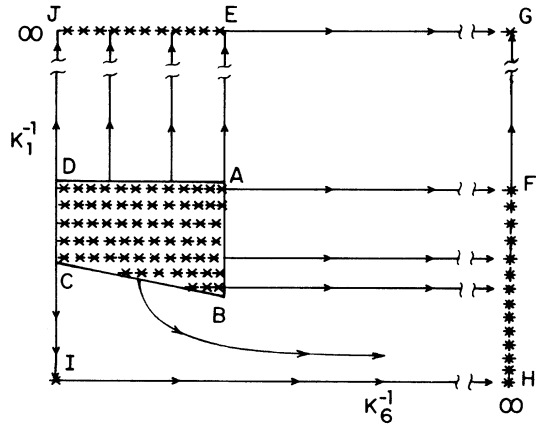

FIG. 3. Schematic renormalization-group flows describing different smectic fluid phases. Asterisks indicate fixed points. In addition to isolated fixed points, there are fixed lines *JE* and *FH*, and fixed surface *ABCD*.

Disclinations, vortices, and the h coupling term are irrelevant inside the trapezoid, and the long-wavelength properties of the resulting state (C^* phase) should be describable by an effective Hamiltonian

$$\bar{H} = \tfrac{1}{2} \int d^2r \, [K_6^R (\vec{\nabla}\theta)^2 + K_1^R (\vec{\nabla}\phi)^2 + 2g_R (\vec{\nabla}\theta)\cdot(\vec{\nabla}\phi)] \quad , \tag{2.29}$$

where K_6^R, K_1^R, and g^R are renormalized versions of the couplings appearing in Eqs. (1.1) and (2.1). The inequalities (1.12)–(1.14) follow directly from the conditions that λ_1, λ_6, and λ_h be negative.

Since correlations can be determined by integrating freely over θ and ϕ in this phase, it is easy to verify the results (1.7a) and (1.7b) quoted in the introduction. All three stiffness constants in Eq. (2.29) could, in principle, be determined by measuring the algebraic falloff of correlations indicated in Eq. (1.4), together with the decay of the four-point function C_Δ discussed in the introduction.

The cross correlation function, $C_\times(r) \equiv \langle \exp[6i\theta(r) - 6i\phi(0)] \rangle$, is more complicated. If $C_\times$ is evaluated at the fixed point, when $h=0$, we simply find $C_\times = 0$, since the Hamiltonian then contains no term which depends on the overall phase difference between ϕ and θ. Nevertheless, at any finite length scale, the renormalized value of h is finite, and we expect to find a nonzero result. The evaluation of $C_\times$ in this phase is carried out in Appendix B.

In analogy to the universal jump prediction for the stiffness in the xy model,[21] we expect that $K_6^R = 2/\pi$ just inside the line *AB* of Fig. 3, and that $K_h^R = 2/\pi$ just inside *BC*. These stiffnesses should approach their universal values with square-root cusp singularities.[24] Such conditions are not enough to completely determine η_1 and η_6, if g_R is unspecified, so these exponents should be nonuniversal on these lines. The exponent η_Δ equals $\frac{1}{4}$ on BC. The stiffness K_6^R is infinite on *CD*, while K_1^R varies smoothly from $9/2\pi$ at C to $2/\pi$ at D on this line.

The arrows in Fig. 3 show schematically our expectations for renormalization-group flows in K_6^{-1} and K_1^{-1} outside the stable trapezoid. Flows immediately above *AD*, which is a locus of vortex-unbinding transitions, should tend toward a fixed line *JE* at $K_1 = 0$. The physics on this fixed line is just that discussed for the hexatic phase in Ref. 5; correlations in the $\theta(\vec{r})$ should be describable by a Hamiltonian of the form

$$\bar{H}_0 = \tfrac{1}{2} \int d^2r \, K_6 (\vec{\nabla}\theta)^2 \quad . \tag{2.30}$$

Disclinations must still be included in the θ field.[5] On the line segment *JE*, disclinations are bound in pairs and may be neglected at large length scales. At point *E*, however, disclination unbind, driving an

instability into a liquid phase described by the fixed point G. The domain of attraction of the fixed line JE determines an untilted hexatic phase, with the properties (1.3) quoted in the Introduction.

Unstable flows immediately to the right of AB are triggered by a disclination unbinding, and should tend toward the fixed line FH at $K_A=0$. This fixed line describes smectic-C liquid-crystal films, with power-law decay in tilt-angle correlations, and a vortex-unbinding transition at F. In an analogy to Eq. (2.30), we expect that correlations in the $\theta(\vec{r})$ are given by a Hamiltonian

$$\bar{H}_0=\frac{1}{2}\int d^2r\, K_1(\nabla\phi)^2 \tag{2.31}$$

provided vortices are also taken into account.

There is, however, *induced* quasi-long-range order in bond-angle correlations in the C phase. To describe bond-angle order, we must add the periodic coupling between the θ and ϕ fields to Eq. (2.31)

$$\bar{H}_0\rightarrow\bar{H}=\bar{H}_0+h\int d^2r\cos[6\theta(\vec{r})-6\phi(\vec{r})]\ . \tag{2.32}$$

This addition has no effect on tilt-angle correlations, since the periodic term disappears when integrated over $\theta(\vec{r})$. In the language of renormalization theory, h is a "redundant" coupling. Consider, though,

$$C_6(\vec{r})\equiv\langle\exp\{6i[\theta(\vec{r})-\theta(\vec{0})]\}\rangle_{\bar{H}}\ , \tag{2.33}$$

where $\langle\ \rangle_{\bar{H}}$ means an average evaluated in the ensemble specified by $\bar{H}$. One finds immediately after a simple change of variables that

$$C_6(\vec{r})=A^2(h)\langle\exp\{6i[\phi(\vec{r})-\phi(\vec{0})]\}\rangle_{\bar{H}_0}\ , \tag{2.34}$$

where

$$A(h)=\frac{\int_{\pi/6}^{\pi/6}d\theta\exp(6i\theta)\exp(h\cos6\theta)}{\int_{-\pi/6}^{\pi/6}d\theta\exp(h\cos6\theta)}\ . \tag{2.35}$$

Below F, where vortices can be neglected, one finds immediately from Eqs. (2.34) and (2.31) that

$$C_6(\vec{r})\simeq A^2(h)r^{-36\eta_1}\ , \tag{2.36}$$

where η_1 is defined by Eq. (1.4). Similar manipulations suffice to show that

$$C_x(\vec{r})\equiv\langle\exp\{6i[\theta(r)-\phi(0)]\}\rangle\simeq A(h)r^{-36\eta_1} \tag{2.37}$$

so one has $\eta_6=\eta_x=36\eta_1$, as claimed in the Introduction. This property of induced order in bond angle correlations should be a quite general feature of smetic-C liquid crystals in two and three dimensions.

In principle, the Hamiltonian (2.30) appropriate to the hexatic phase should also be replaced with something analogous to Eq. (2.32). There are *no* induced tilt-angle correlations, however, since one now finds a result like Eq. (2.34) for C_1, with Eq. (2.35) replaced by a quantity which vanishes identically,

$$A'(h)=\frac{\int_{-\pi/6}^{\pi/6}d\phi\exp(i\phi)\exp(h\cos6\phi)}{\int_{-\pi/6}^{\pi/6}d\phi\exp(h\cos6\phi)}=0\ . \tag{2.38}$$

This result is consistent with the exponential decay of $C_1(\vec{r})$ quoted in the Introduction for the hexatic phase.

Finally, we discuss the unstable flows just below CB in Fig. 3, which are triggered by an unbinding of the periodic excitations in Eq. (2.17). As discussed in Sec. II A, the line IH at $K_1=\infty$ is like the xy model in a magnetic field, with fixed points at $K_6=0$ and $K_6=\infty$. Indeed, the flows immediately below CB may ultimately tend toward the fixed line FH, and the phase below this line could just be part of the smectic-C phase discussed above.

To study this point further, consider the Hamiltonian (2.1) in the absence of disclinations and vortices. This should be a good approximation near CB. Equation (2.1) then simplifies upon defining fields $\theta_\pm(\vec{r})$,

$$\theta_+(\vec{r})=\alpha\theta(\vec{r})+\beta\phi(\vec{r})\ , \tag{2.39a}$$

$$\theta_-(\vec{r})=\theta(\vec{r})-\phi(\vec{r})\ , \tag{2.39b}$$

where

$$\alpha=(1-\beta)=\frac{K_6+g}{K_6+K_1+2g}\ . \tag{2.40}$$

In terms of the $\theta_\pm(\vec{r})$, the Hamiltonian breaks into a sum of a Gaussian in $\vec{\nabla}\theta_+$ and "sine-Gordon" Hamiltonian in θ_-,

$$\bar{H}=\frac{1}{2}\int d^2r\,(K_+|\vec{\nabla}\theta_+|^2+K_-|\vec{\nabla}\theta_-|^2)+h\int d^2r\cos(p\theta_-)\ , \tag{2.41}$$

with

$$K_+=K_6+K_1+2g\ , \tag{2.42a}$$

$$K_-=(K_1K_6-g^2)/K_+=9/\pi^2K_h\ . \tag{2.42b}$$

We can now determine bond- and tilt-angle correlations using the known properties of the "sine-Gordon" problem.[20,26,27] In particular, one expects long-range order in $\exp[iq\theta_-(\vec{r})]$, where q is arbitrary, provided K_- is large enough so that we are below the line CB in Fig. 3,

$$\lim_{r\rightarrow\infty}\langle\exp[iq\theta_-(\vec{r})]\exp[-iq\theta_-(\vec{0})]\rangle=\text{const}\neq0\ . \tag{2.43}$$

Correlations in $\exp[iq\theta_+(\vec{r})]$, on the other hand,

are always algebraic in these regions. Since Eqs. (2.39) can be inverted to read

$$\phi(\vec{r}) = \theta_+(\vec{r}) - \alpha\theta_-(\vec{r}) \ , \tag{2.44a}$$

$$\theta(\vec{r}) = \theta_+(\vec{r}) + \beta\theta_-(\vec{r}) \ , \tag{2.44b}$$

it is straightforward to determine $C_6(\vec{r})$, $C_1(\vec{r})$, and $C_x(\vec{r})$ at large distances using the properties quoted above. Below the line CB all these correlations decay as power laws, with

$$\eta_6 = \eta_x = 36\eta_1 = 18/\pi K_+ \ . \tag{2.45}$$

Since this is also the behavior we associated with the fixed line FH, this phase may be indentical with the C phase described above. On the other hand, we cannot rule out a first-order transition, separating C_1 and C_2 phases with the same symmetry.

C. Weak-coupling recursion relations

We now study the neighborhood of the special points A and B in Fig. 3, using renormalization equations constructed as expansions in the fugacities y_6, y_1, and y_h. Since only two of these fugacities become relevant near A and B (for $p > 4$), we shall supress one "irrelevant" set of excitations. One is left with two coupled scalar Coulomb gases. (Away from A and B, and in particular near the lines AD, AB, and BC, at most one set of excitations is important, and one can then take over the results of Kosterlitz[24] for a single scalar Coulomb gas.)

Consider first recursion relations valid near the point A of Fig. 3. The coupling y_h may be set equal to zero in this region, and the Hamiltonian (2.17) simplifies to

$$\bar{H} = \bar{H}_c\left(\frac{K_6}{p^2}, y_6, \{m\}\right) + \bar{H}_c(K_1, y_1, \{n\}) + \frac{2\pi g}{p} \sum_{\vec{r}' \neq \vec{r}} m(\vec{r})\, n(\vec{r}\,') \ln\left(\frac{|\vec{r} - \vec{r}\,'|}{a}\right) \ . \tag{2.46a}$$

The corresponding partition sum is

$$Z = (\text{const}) \sum_{\{m(\vec{r})\}}{}' \sum_{\{n(\vec{r})\}}{}' e^{\bar{H}} \ . \tag{2.46b}$$

The couplings K_6, y_6, K_1, y_1, and g are altered slightly from their values in Eq. (2.17) by the supressed $\{s(\vec{r})\}$ excitations. In particular, the $\{s(\vec{r})\}$ generate a nonzero value of g even if this coupling is initially zero.

Recursion formulas appropriate to Eq. (2.46a) are constructed in Appendix A, using the method of Kosterlitz[24] and of Anderson and Yuval.[28] Upon scaling up the core diameters of disclinations and vortices from a to ae^l in Eq. (2.46), we find an effective Hamiltonian like Eq. (2.46a), but with renormalized couplings $K_6(l)$, $y_6(l)$, $K_1(l)$, $y_1(l)$, and $g(l)$. These couplings are solutions of differential recursion relations, which, to leading order in $y_6(l)$ and $y_1(l)$, read

$$\frac{dK_6}{dl} = \frac{-4\pi^3}{p^2} K_6^2 y_6^2 - 4\pi^3 g^2 y_1^2 \ , \tag{2.47a}$$

$$\frac{dy_6}{dl} = \left(2 - \frac{\pi K_6}{p^2}\right) y_6 \ , \tag{2.47b}$$

$$\frac{dK_1}{dl} = -4\pi^3 K_1^2 y_1^2 - \frac{4\pi^3}{p^2} g^2 y_6^2 \ , \tag{2.47c}$$

$$\frac{dy_1}{dl} = (2 - \pi K_1) y_1 \ , \tag{2.47d}$$

$$\frac{dg}{dl} = 0 \ . \tag{2.47e}$$

Note that, with y_h set to zero, $g(l)$ remains fixed at its initial value to this order.

To study the system (2.47) near $K_4 \simeq 2p^2/\pi$ and $K_1 \simeq 2/\pi$, it is helpful to study deviations $x_a(l)$ and $x_b(l)$ defined by

$$K_6^{-1}(l) \equiv \frac{\pi}{2p^2}[1 + x_a(l)] \ , \tag{2.48a}$$

$$K_1^{-1}(l) \equiv \tfrac{1}{2}\pi[1 + x_b(l)] \ , \tag{2.48b}$$

as well as rescaled fugacities

$$y_a^2(l) \equiv 8\pi^2 y_6^2(l) \ , \tag{2.48c}$$

$$y_b^2(l) \equiv 8\pi^2 y_1^2(l) \ .$$

To lowest order in these variables, the recursions relations (2.47a)–(2.47d) become

$$\frac{dx_a}{dl} = y_a^2 + \gamma y_b^2 \ , \tag{2.49a}$$

$$\frac{dy_a}{dl} = 2x_a y_a \ , \tag{2.49b}$$

$$\frac{dx_b}{dl} = y_b^2 + \gamma y_a^2 \ , \tag{2.49c}$$

$$\frac{dy_b}{dl} = 2x_b y_b \ , \tag{2.49d}$$

with

$$\gamma = \pi^2 g^2 / 2p^2 \ . \tag{2.49e}$$

Although the flows generated by the system (2.49) are complicated, it is easily checked that the quantity

$$C \equiv 2x_a^2(l) + 2x_b^2(l) - 4\gamma x_a(l) x_b(l) - (1 - \gamma^2)[y_a^2(l) + y_b^2(l)] \tag{2.50}$$

is invariant along the trajectories,

$$\frac{dC}{dl} = 0 \ . \tag{2.51}$$

Since C is entirely determined by Eq. (2.50) evaluated at $l=0$, it is an analytic function of the initial conditions.

The detailed phase diagram near A in Fig. 3 suggested by these recursion relations is shown in Fig. 4. Both $y_a(l)$ and $y_b(l)$ ultimately tend to zero in the shaded unlocked-tilted-hexatic phase. A line AD of vortex unbindings is determined by a locus of initial conditions such that $y_a(l)\to 0$, $y_b(l)\to 0$, and $x_b(l)\to 0$ as l tends to infinity. In this case, we have from Eq. (2.50) the requirement

$$C=2x_a^2(\infty)\ , \tag{2.52a}$$

where $x_a(\infty)=\lim_{l\to\infty}x_a(l)$. Similarly, the requirement

$$C=2x_b^2(\infty) \tag{2.52b}$$

determines a line of disclination unbindings AB. These two lines intersect at A, where

$$x_a(\infty)=x_b(\infty)=0\ . \tag{2.52c}$$

According to the recursion formulas (2.47a) and (2.47c), *both* $K_6(l)$ and $K_1(l)$ are destabilized and pushed toward smaller values when $y_6(l)$ starts to grow. This happens whenever $K_6\lesssim 2p^2/\pi$. Since this double instability also occurs when $y_1(l)$ becomes unstable, we expect a portion A_1AA_2 of the unlocked-tilted-hexatic phase boundary when disclinations and vortices unbind simultaneously. In the limit $g=0$, this region shrinks to a point.

The hexatic-liquid phase boundary A_1E can be determined as follows. Assume initial conditions in the hexatic phase just above A_1D, so that vortices have unbound. The recursion relations can then be integrated until one is far enough from A_1D, to treat the unbound vortices using a "Debye-Hückel" approximation[29]: the vortex degrees of freedom must be sufficiently excited to allow one to integrate rather than sum over the integers $\{n\}$ in Eq. (2.46b).

Let us assume that this condition is satisfied when $l=l^*$ such that $K_1(l^*)$ equals, say, π^{-1}, twice its critical value. In terms of the Fourier-transformed integer fields

$$\hat{m}(\vec{q})=\sum_{\vec{r}}\exp(i\vec{q}\cdot\vec{r})m(\vec{r})\ , \tag{2.53a}$$

$$\hat{n}(\vec{q})=\sum_{\vec{r}}\exp(i\vec{q}\cdot\vec{r})m(\vec{r})\ , \tag{2.53b}$$

the Hamiltonian (2.46a) becomes

$$\begin{aligned}\bar{H}=&-\tfrac{1}{2}\int_q\left(\frac{4\pi^2K_6}{q^2p^2}+B_6\right)\hat{m}(\vec{q})\hat{m}(-\vec{q})\\&-\tfrac{1}{2}\int_q\left(\frac{4\pi^2K_1}{q^2}+B_1\right)\hat{n}(\vec{q})\hat{n}(-\vec{q})\\&-\tfrac{1}{2}\int_q\frac{4\pi^2g}{q^2p}[\hat{m}(\vec{q})\hat{n}(-\vec{q})+\hat{m}(-\vec{q})\hat{n}(-\vec{q})]\ ,\end{aligned} \tag{2.54}$$

where B_6 and B_1 are constants depending on the fugacities y_6 and y_1, and on the cutoff. Integrating freely over the vortex field $\hat{n}(\vec{q})$ when $l=l^*$, we find an effective Hamiltonian for disclinations of the form

$$\bar{H}_{\rm eff}=-\tfrac{1}{2}\int_q\left(\frac{4\pi^2K_6^{\rm eff}}{q^2p^2}+B_6^{\rm eff}+O(q^2)\right)\hat{m}(\vec{q})\hat{m}(-\vec{q})\ , \tag{2.55a}$$

with

$$K_6^{\rm eff}=K_6(l^*)-g^2/K_1(l^*) \tag{2.55b}$$

and a similar expression for $B_6^{\rm eff}$. Rewriting Eq. (2.55) in terms of the $\{m(\vec{r})\}$, we find a Coulomb gas like Eq. (2.18) with $K=K_6^{\rm eff}/p^2$ and an effective fugacity $y_6^{\rm eff}$. The disclinations will unbind when $K_6^{\rm eff}\simeq 2/\pi p^2$, a requirement which determines the line A_1E.

Evidently, the effect of the cross coupling g is to *depress* the disclination unbinding temperature. Physically, we can imagine oppositely charged "red" and "blue" vortices coexisting with bound disclination pairs. Because of the logarithmic interaction proportional to g in Eq. (2.46a), plus disclinations will be screened by a cloud of, say, red vortices, and minus disclinations screened by a cloud of blue ones. This reduces the strength of the logarithmic interaction between disclination pairs, and lowers T_c.

A very similar treatment applies to the unstable flows to the right of the line AB in Fig. 4. Integrating now until $K_6(l^*)$ equals, say, twice its critical value, and treating disclinations in the Debye-Hückel approximation, one obtains an effective Coulomb gas for vortex excitations with

$$K_1^{\rm eff}=K_1(l^*)-g^2/p^2K_6(l^*)\ . \tag{2.56}$$

Vortices will unbind when $K_6^{\rm eff}\simeq 2/\pi$ (this deter-

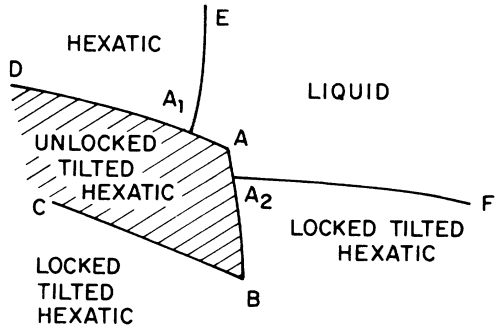

FIG. 4. More detailed version of the region surrounding the point A in Fig. 3. Four possible fluid phases are indicated.

mines the line A_2F), and the transition temperatures are again reduced due to vortex-disclination interactions.

It is interesting to consider the behavior of the susceptibilities

$$\chi_6 \equiv \int d^2r\, C_6(\vec{r}) \ , \tag{2.57a}$$

$$\chi_1 \equiv \int d^2r\, C_1(\vec{r}) \ , \tag{2.57b}$$

when approaching the different transition lines in Fig. 4. Results can be extracted in a straightforward manner from our recursion relations using the method of Kosterlitz.[24] Although χ_6 may be difficult to measure, χ_1 can be probed directly in light-scattering experiments. When the lines AD or AA_2 are approached in the hexatic or liquid phases, one finds

$$\chi_1 \simeq \xi_+^{2-\eta_1^*} \ , \tag{2.58}$$

where η_1^* is the exponent defined by Eq. (1.4) at the point being crossed. The correlation length $\xi_+(T)$ has the temperature dependence found by Kosterlitz,[24]

$$\xi_+(T) \simeq \exp(b/t^{1/2}) \ , \tag{2.59}$$

where t is the deviation from the critical temperature, $t=(T-T_c)/T_c$. The susceptibility χ_6 is infinite in the hexatic phase, but upon crossing AA_1 or AB from the liquid or unlocked-tilted-hexatic phases, one has for the singular part of χ_6,

$$\chi_6 \simeq \xi_+^{2-\eta_6^*} \ , \tag{2.60}$$

where η_6^* is the exponent of the point being crossed. Even though C_6 decays algebraically to zero in the C phase, χ_6 is finite then, provided $\eta_6 = 36\eta_1 \gtrsim 2$. Both susceptibilities are infinite in the unlocked-tilted-hexatic phase. The quantity χ_6 diverges like $\xi_+^{7/4}$ upon crossing A_1E from the liquid side, while χ_1 remains finite. Similarly, χ_1 behaves like $\xi_1^{7/4}$ upon crossing A_2F, while χ_6 remains finite. As usual,[24] there are only experimentally undetectable essential singularities in the specific heat on all the above transition lines.

Finally, we consider briefly recursion relations near the point B in Fig. 3. Here, we can neglect vortices, and Eq. (2.17) can be replaced by

$$\bar{H} = \bar{H}_c(K_h, y_h, \{s\}) + \bar{H}_c\left(\frac{K_6}{p^2}, y_6, \{m\}\right) + i \sum_{\vec{r}\neq\vec{r}'} s(\vec{r})\, m(\vec{r}') \tan^{-1}\left(\frac{y-y'}{x-x'}\right) \ , \tag{2.61}$$

with slightly altered parameters K_h, y_h, K_6, and y_6. According to Appendix A, the recursion relations for this problem are

$$\frac{dK_6}{dl} = -\frac{4\pi^3}{p^2} K_6^2 y_6^2 + p^2 y_h^2 \ , \tag{2.62a}$$

$$\frac{dy_6}{dl} = 2 - \left(\frac{\pi K_6}{p^2}\right) y_6 \ , \tag{2.62b}$$

$$\frac{dK_h}{dl} = -4\pi^3 K_h^2 y_h^2 + \pi y_6^2 \ , \tag{2.62c}$$

$$\frac{dy_h}{dl} = (2 - \pi K_h) y_h \ . \tag{2.62d}$$

These formulas may be analyzed near B just as was done for the recursion near A. One recovers the transition lines BC and BA, and finds that χ_6 diverges as in Eq. (2.60). The quantity χ_1 is infinite in both tilted hexatic phases.

The Debye-Hückel approximation is more difficult to carry out here, because of subtleties associated with the invariance of the inverse tangent part of $e^{\bar{H}}$ to transformations like $s(\vec{r}) \to s(\vec{r}) + 2\pi$ and $m(\vec{r}) \to m(\vec{r}) + 2\pi$.

D. Strong coupling

There is one remaining limit in which the Hamiltonian (2.1) simplifies: the limit of infinite h. To study this situation, we rewrite Eq. (2.1) in a form which makes manifest its periodicity as a function of θ and ϕ,

$$\bar{H} = \frac{K_6}{p^2} \sum_{\langle \vec{r}, \vec{r}' \rangle} \cos[p\theta(\vec{r}) - p\theta(\vec{r}')] + K_1 \sum_{\langle \vec{r}, \vec{r}' \rangle}{}' \cos[\phi(\vec{r}) - \phi(\vec{r}')] + \frac{g}{p} \sum_{\langle \vec{r}, \vec{r}' \rangle} \sin[p\theta(\vec{r}) - p\theta(\vec{r}')] \sin[\phi(\vec{r}) - \phi(\vec{r}')] + h \sum_{\vec{r}} \cos[p\theta(\vec{r}) - p\phi(\vec{r})] \ , \tag{2.63}$$

where $\sum'_{\langle \vec{r}, \vec{r}' \rangle}$ denotes a sum over nearest-neighbor sites on, say, a square lattice. This expression reduces to Eq. (2.1) in the continuum limit, and displays particularly simple periodic interactions between adjacent lattice sites.

When h is infinite the functional integrals in Eq. (2.2) become restricted to complexions such that

$$\theta(\vec{r}) = \phi(\vec{r}) + 2\pi s(\vec{r})/p \ , \tag{2.64}$$

where $s(\vec{r})$ is an integer which can vary from site to site. The partition sum is then

$$Z = (\text{const}) \int D\phi \, e^{\bar{H}_\infty} \ , \tag{2.65a}$$

where

$$\bar{H}_\infty = \sum_{\langle \vec{r}, \vec{r}' \rangle} \left[\frac{K_6}{p^2} \cos[p\phi(\vec{r}) - p\phi(\vec{r}')] + K_1 \cos[\phi(\vec{r}) - \phi(\vec{r}')] + \frac{g}{p} \sin[p\phi(\vec{r}) - p\phi(\vec{r}')] \sin[\phi(\vec{r}) - \phi(\vec{r}')] \right] \tag{2.65b}$$

and the dependence on the $\{s(\vec{r})\}$ has dropped out. This Hamiltonian can be thought of as representing an xy model of magnetism, with a particularly complicated periodic interaction between nearest neighbors.

Although we have not studied Eq. (2.65b) in detail (this could be done using the Migdal approximate recursion formula,[30,31] for example), a qualitatively correct phase diagram follows from considering different limiting cases. For sufficiently small K_6 and K_1, both $C_6(\vec{r})$ and $C_1(\vec{r})$ should decay exponentially in an isotropic fluid phase. In the limit $K_1 \to 0$, g must also tend to zero if, for simplicity, we impose the restriction (2.3). Equation (2.65b) then exhibits an unbinding of $\frac{1}{6}$ - integer vortices in the θ field, by virtue of Eq. (2.64). For small K_6^{-1}, we expect a hexatic phase, with power-law decay of $C_6(\vec{r})$, and exponential decay of $C_1(\vec{r})$. If $K_6 = 0$, however, integer vortices unbind for large enough K_1^{-1}. For K_1^{-1} small, it is easily shown that correlations exhibit the locked algebraic decay (with $\eta_6 = \eta_x = 36\eta_1$) we identified earlier with a locked-tilted-hexatic (smectic-C) phase.

Finally, consider the limit $K_6 \to \infty$. One then has

$$\phi(\vec{r}) = \phi_0 + \frac{2\pi}{p} t(\vec{r}) \ , \tag{2.66}$$

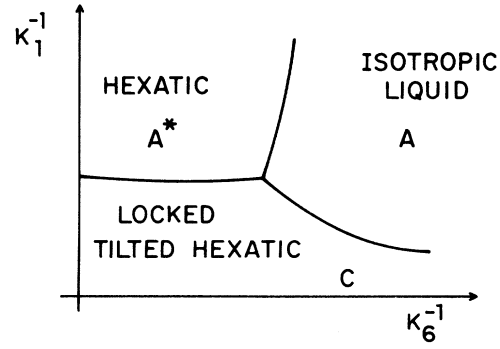

FIG. 5. Possible fluid phase diagram in the strong-coupling ($h = \infty$) limit. The unlocked tilted phase, which is not shown, may not exist in this limit.

where $t(r)$ is an integer field, and the partition sum becomes

$$Z = (\text{const}) \sum_{\{t(\vec{r})\}} \exp\left[K_1 \sum_{\langle \vec{r}, \vec{r}' \rangle} \cos\left(\frac{2\pi t(\vec{r})}{p} - \frac{2\pi t(\vec{r}')}{p} \right) \right] . \tag{2.67}$$

This is the p-state clock model considered by José *et al.*[20] The Migdal recursion formula and perturbative renormalization-group analysis[20] suggest that these models have two phase transitions for p greater than a critical value p_c. Although $p_c = 4$ in a weak-coupling approximation,[20] this critical value is not known precisely for the Hamiltonian (2.67). For $p = 6$, there could be a single phase transition from a phase with exponential decay of $C_1(\vec{r})$ to a phase with long-range order $\langle \exp[i\theta(\vec{r})] \rangle \neq 0$, and locked long-range order in $\exp[6i\theta(\vec{r})]$. For any finite K_6, long-range order in $\exp[i\phi(\vec{r})]$ and $\exp[6i\theta(\vec{r})]$ is impossible.

A tentative phase diagram consistent with these observations is shown in Fig. 5. Hexatic, liquid, and locked-tilted-hexatic phases are shown. Although the unlocked-tilted-hexatic phase is absent, we cannot be positive that this is indeed the case in the strong-coupling limit.

III. SOLID PHASES

The starting Hamiltonian for investigation of the solid phases is Eq. (1.16) above. We shall assume that the elastic constants are sufficiently large so that dislocations are bound, and shall investigate the possibilities for the tilt orientation parameter, $\Phi(\vec{r}) = (\sin\gamma) e^{i\phi(\vec{r})}$. For a rigid lattice, $u_{ij} = 0$, and we need only consider the coupling h of ϕ to the hexagonal asymmetry, plus the effects of vortices in the ϕ field, which have not been written explicitly in Eq. (1.16). As discussed in Ref. 20, three phases are possible for this system, at least if the bare value of h is not too large. At intermediate temperatures, an xy-like phase occurs, with quasi-long-range order in

the correlation function $C_1(\vec{r})$. For the phase to be stable, the exponent η_1 must lie in the range

$$\tfrac{1}{9} < \eta_1 < \tfrac{1}{4} \quad . \tag{3.1}$$

At high temperatures, where η_1 exceeds $\frac{1}{4}$, the system is unstable to vortex formation, and a paramagnetic phase results, with exponential decay of $C_1(\vec{r})$. For low temperatures, where η_1 is less that $\frac{1}{9}$, the coupling h becomes a "relevant perturbation", and the order parameter is locked to one of the six easy axes, $\langle e^{i\phi}\rangle \neq 0$. The three phases of the tilted molecules on a rigid lattice are indicated in Fig. 6.

We now show that for a nonrigid lattice this intermediate phase is destabilized by the "magnetoelastic" term in Eq. (1.16). To see this, consider the renormalized elastic constants determined from the Hamiltonian appropriate to the intermediate phase,

$$\bar{H}_I = \tfrac{1}{2}\int d^2r\,(2\mu u_{ij}^2 + \lambda u_{kk}^2) + w\int d^2r\,(u_{ij} - \tfrac{1}{2}\delta_{ij}u_{kk})s_i s_j + \tfrac{1}{2}K_1\int d^2r\,(\vec{\nabla}\phi)^2 \quad . \tag{3.2}$$

The inverse tensor of renormalized elastic constant may be written

$$(C_R^{-1})_{ijkl} = (\langle U_{ij}U_{kl}\rangle - \langle U_{ij}\rangle\langle U_{kl}\rangle)/A \quad , \tag{3.3}$$

where

$$U_{ij} = \int d^2r\, u_{ij}(\vec{r}) \tag{3.4}$$

and A is the area of the system. Terms linear in u_{ij} in $\bar{H}_I$ may be eliminated upon defining a new strain field,

$$\tilde{u}_{ij} = u_{ij} + \frac{w}{2\mu}(s_i s_j - \tfrac{1}{2}\delta_{ij}) \tag{3.5}$$

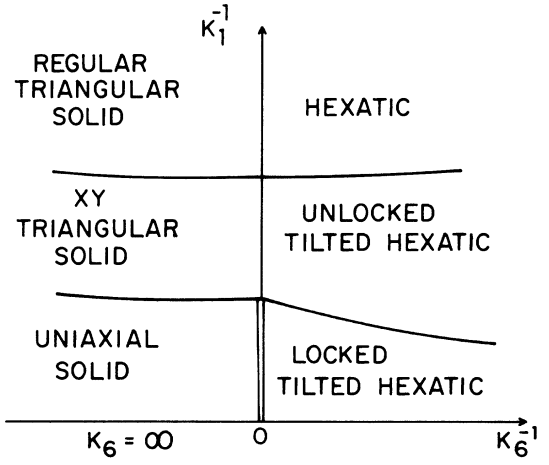

FIG. 6. Solid and fluid phases when the coupling w of the orientational order parameter to the elastic degrees of freedom is negligible. The xy triangular solid phase is unstable when this coupling in nonzero.

in terms of which $\bar{H}_I$ becomes

$$\bar{H}_I = (\text{const}) + \tfrac{1}{2}\int d^2r\,(2\mu\tilde{u}_{ij}^2 + \lambda\tilde{u}_{kl}^2) + \tfrac{1}{2}K_1\int d^2r\,(\vec{\nabla}\phi)^2 \quad . \tag{3.6}$$

The elastic tensor is then

$$(C_R^{-1})_{ijkl} = \frac{\langle \tilde{U}_{ij}\tilde{U}_{kl}\rangle}{A} + \frac{w^2}{4\mu^2 A}(\langle S_{ij}S_{kl}\rangle - \langle S_{ij}\rangle\langle S_{kl}\rangle) \quad , \tag{3.7}$$

where

$$\tilde{U}_{ij} = \int d^2r\,\tilde{u}_{ij}(\vec{r}) \quad , \quad S_{ij} = \int d^2r\, s_i(\vec{r})s_j(\vec{r}) \quad . \tag{3.8}$$

Substituting Eq. (3.8) into Eq. (3.7), it is now straightforward to evaluate the averages in Eq. (3.13) and find

$$(C_R^{-1})_{ijkl} = \frac{1}{4\mu}(\delta_{ik}\delta_{jl} + \delta_{il}\delta_{jk}) - \frac{\lambda}{4\mu(\mu+\lambda)}\delta_{ij}\delta_{kl} + \frac{w^2}{4\mu^2}I(K_1)(\delta_{ik}\delta_{jl} + \delta_{il}\delta_{jk} - \delta_{ij}\delta_{kl}) \quad , \tag{3.9}$$

where

$$I(K_1) = \int d^2r\,\langle \exp[2i\phi(\vec{r}) - 2i\phi(\vec{0})]\rangle \quad . \tag{3.10}$$

Although the elastic part of the bulk modulus is unaffected,

$$(\mu_R + \lambda_R)^{-1} = (C_R^{-1})_{iijj} = (\mu+\lambda)^{-1} \quad , \tag{3.11}$$

the magnetoelastic coupling does alter the shear modulus,

$$\mu_R^{-1} = (C_R^{-1})_{ijij} - \tfrac{1}{2}(C_R^{-1})_{iijj} = \frac{1}{\mu}[1 + w^2 I(K_1)] \quad . \tag{3.12}$$

Since one readily finds that

$$I(K_1) \simeq 2\pi\int_a^\infty dr\, r^{1-\eta_2} \quad , \tag{3.13}$$

where

$$\eta_2 = 2/\pi K_1^R = 4\eta_1 < 1 \quad , \tag{3.14}$$

the renormalization of μ_R^{-1} is infinite.

Thus, μ_R vanishes, and the intermediate xy-like phase in Fig. 6 is unstable to shear distortions. In the language of the renormalization group the eigenvalue of w is

$$\lambda_w = 1 - \tfrac{1}{2}\eta_2 \quad , \tag{3.15}$$

which is relevant (positive) in the intermediate phase.

The shear instability of the xy-like phase, leads, presumably, to a distorted lattice, in which there is a nonzero value of $\langle e^{i\phi}\rangle$, as well as a uniform shear strain

$$\langle u_{ij}\rangle \approx \frac{-w}{2\mu}(\langle s_i\rangle\langle s_j\rangle - \tfrac{1}{2}\delta_{ij}|\langle\vec{s}\rangle|^2) \quad . \tag{3.16}$$

Of course, the same phase would have resulted if we had added the coupling to lattice distortions directly to the low-temperature ordered phase of Fig. 6. Thus, on the nonrigid lattice, the two lower phases of Fig. 6 will be replaced by a single uniaxial phase, labeled H in Fig. 2. Although this is the simplest possible situation, we cannot, of course, rule out a first-order phase transition between uniaxial phases with the same symmetry.

To investigate the stability of the long-range tilt-angle order in the H phase against fluctuations in ϕ, we return to the full solid-phase free energy (1.16), and expand u_{ij} about its minimum (3.16). We assume for convenience that $\theta_0=0$, that h is positive, and the tilt axis has aligned itself along the x axis, so that $\langle\phi\rangle=0$. We work, for simplicity, at sufficiently low temperatures so that $|\langle\vec{s}\rangle|$ can be replaced by unity. Substituting Eq. (3.16) into Eq. (1.16), and expanding in ϕ, we find, to quadratic order in $\tilde{u}_{ij}$ and ϕ,

$$\frac{H}{k_BT}=\frac{1}{2}\int d^2r\left(2\mu\tilde{u}_{ij}^2+\lambda\tilde{u}_{kk}^2+\frac{1}{2}K_1(\vec{\nabla}\phi)^2+36h\phi^2+\frac{w^2}{\mu}\phi^2+2w\tilde{u}_{xy}\phi\right) . \tag{3.17}$$

Upon Fourier transforming and using Eq. (1.17), this becomes

$$\frac{H}{k_BT}=\frac{1}{2}\int_q\left[(2\mu+\lambda)|q_i\hat{u}_i(\vec{q})|^2+\mu(q^2\delta_{ij}-q_iq_j)\hat{u}_i(\vec{q})\hat{u}_j(-\vec{q})\right.$$
$$\left.+\left(K_1q^2+36h+\frac{w^2}{\mu}\right)\hat{\phi}(\vec{q})\hat{\phi}(-\vec{q})+2iw[q_xu_y(\vec{q})+q_yu_x(\vec{q})]\hat{\phi}(-\vec{q})\right] . \tag{3.18}$$

It follows that

$$\langle|\phi(\vec{q})|^2\rangle=\left[K_1q^2+36h+\frac{4(\mu+\lambda)w^2}{\mu(2\mu+\lambda)}\frac{q_x^2q_y^2}{q^4}\right]^{-1} . \tag{3.19}$$

Fluctuations in $\phi(r)$ may be calculated by taking the Fourier transform of Eq. (3.19)

$$\langle|\phi(\vec{r})|^2\rangle=\int\frac{d^2q}{(2\pi)^2}\langle|\phi(\vec{q})|^2\rangle . \tag{3.20}$$

Note that the integral converges, even if $h=0$. Thus, if the renormalized value of w^2/μ is of order unity or larger, fluctuations in $\phi(r)$ will be of order unity or smaller, and we expect that $\langle e^{i\phi}\rangle\neq0$. The resulting phase is a uniaxial solid, labeled H in Fig. 2.

The nature of the transitions between the uniaxial solid phase H and the various adjacent phases in Fig. 2 (B, C, or C^*) has not been determined.

ACKNOWLEDGMENTS

The authors are grateful for discussions with R. J. Birgeneau, S. Hikami, J. D. Litster, P. Pershan, and R. Pindak. Research has been supported by the NSF through the Harvard Material Research Laboratory and through Grant No. DMR77-10210.

APPENDIX A: DERIVATION OF SCALING EQUATIONS

In this appendix, we outline a derivation of the renormalization-group or "scaling" recursion equations used in the text. Consider first recursion relations valid near the point B in Fig. 4. We shall discuss a generalization of the Hamiltonian (2.61), namely,

$$\bar{H}=\bar{H}_c(K_a,y_a,\{m\})+\bar{H}_c(K_b,y_b,\{n\})$$
$$+iq\sum_{\vec{r}\neq\vec{r}'}m(\vec{r})n(\vec{r})\tan^{-1}\left(\frac{y-y'}{x-x'}\right) , \tag{A1}$$

where q is an integer. With $q=1$, $K_a=K_6/p^2$, $y_a=y_6$, $K_b=K_h$, and $y_b=y_h$, this reduces to Eq. (2.61). For $K_a=q^2/4\pi^2K_b\equiv K$, however, it reduces to a representation of an xy model with vortices and a $\cos(p\theta)$ crystal field obtained by Kadanoff.[25] The partition sum

$$Z=\sum_{\{m\}}{}'\sum_{\{s\}}{}'e^{\bar{H}} \tag{A2}$$

then has the self-duality property

$$Z(K,y_a,y_b)\propto Z(q^2/4\pi^2K,y_b,y_a) \tag{A3}$$

(where the proportionality constant is a smooth function of K), discussed by Jose *et al.*[20] Our recursion formulas should agree with the known results[20] in this special case.

Following Kosterlitz[24] and Anderson and Yuval,[28] we restrict our attention to excitations with charges ±1, and expand Z in a power series in y_a and y_b

$$Z=\sum_{M=0}^{\infty}\sum_{N=0}^{\infty}\left(\frac{1}{M!}\right)^2\left(\frac{1}{N!}\right)^2y_a^{2M}y_b^{2N}Z_{M,N} . \tag{A4}$$

It will be convenient in what follows to call the $\{m\}$ and $\{n\}$ excitations green and white "vortices,"

respectively. The quantity $Z_{M,N}$ is then the configurational partition sum for $2M$ green and $2N$ white vortices,

$$Z_{M,N}=\left[\prod_{i=1}^{2M}\int' d^2r_i\right]\left[\prod_{j=1}^{2N}\int' d^2R_j\right]e^{\bar{H}_{M,N}} , \quad \text{(A5a)}$$

with

$$\bar{H}_{M,N}=2\pi K_a\sum_{i\neq j}G(\vec{r}_i-\vec{r}_j)m(\vec{r}_i)m(\vec{r}_j) +2\pi K_b\sum_{i\neq j}G(\vec{R}_i-\vec{R}_j)n(\vec{R}_i)n(\vec{R}_j) +2iq\sum_{i\neq j}\tilde{G}(\vec{r}_i-\vec{R}_j)m(\vec{r}_i)n(\vec{R}_j) , \quad \text{(A5b)}$$

and where the $\{\vec{r}\}$ denote $2M$ green vortices, and the $\{\vec{R}_j\}$ signify $2N$ white ones. The green and white vortices each obey charge neutrality. Each integration in Eq. (A5) is excluded from circles of radius a about all others vortices, and the functions $G(\vec{r})$ and $\tilde{G}(\vec{r})$ are harmonic conjugates,

$$G(\vec{r})=\ln(|\vec{r}|/a) , \quad \text{(A6)}$$

$$\tilde{G}(\vec{r})=\tan^{-1}\left[\frac{y-y'}{x-x'}\right] . \quad \text{(A7)}$$

A renormalization transformation can now be constructed by integrating over those configurations where two oppositely charged vortices of the same color approach each other with separations between a and ae^{δ}, with δ small. Breaking up in integrations in Eq. (A5) in this way, we can write, to leading order in δ

$$\left[\prod_{i=1}^{2M}\int' d^2r_i\right]\left[\prod_{j=1}^{2N}\int' d^2R_j\right]e^{\bar{H}_{M,N}}=\left[\prod_{i=1}^{2M}\int^{>} d^2r_i\right]\left[\prod_{j=1}^{2N}\int^{>} d^2R_j\right]e^{\bar{H}_{M,N}} +\sum_{k=1}^{M}\sum_{l=1}^{M}\left[\prod_{\substack{i=1\\ i\neq k,l}}^{2M}\int^{>} d^2r_i\right]\left[\prod_{j=1}^{2N}\int^{>} d^2R_j\right]\int d^2x\int^{\delta} d^2y\, e^{\bar{H}_{M,N}} +\sum_{r=1}^{N}\sum_{t=1}^{N}\left[\prod_{i=1}^{2M}\int^{>} d^2r_i\right]\left[\prod_{\substack{j=1\\ j\neq t,s}}^{2N}\int^{>} d^2R_j\right]\int d^2X\int^{\delta} d^2Y\, e^{\bar{H}_{M,N}}+O(\delta^2) , \quad \text{(A8)}$$

where the integrals $\int^{>}$ are excluded from circles of radii ae^{δ} around all other vortices, and

$$\vec{x}=\vec{r}_k-\vec{r}_l , \quad \text{(A9)}$$

$$\vec{y}=\tfrac{1}{2}(\vec{r}_k+\vec{r}_l) , \quad \text{(A10)}$$

$$\vec{X}=\vec{R}_s-\vec{R}_t , \quad \text{(A11)}$$

$$\vec{Y}=\tfrac{1}{2}(\vec{R}_s+\vec{R}_t) . \quad \text{(A12)}$$

The second term of Eq. (A8) sums over pairs of oppositely charged green vortices at $\vec{r}_k$ and $\vec{r}_l$, while the third term sums over white charge-neutral pairs at $\vec{R}_s$ and $\vec{R}_t$. These pairs must be within ae^{δ} of each other. The integrations over $\vec{y}$ and $\vec{Y}$ are restricted to annuli of width δ, while the $\vec{x}$ and $\vec{X}$ integrations are essentially unrestricted. Other possible pairings of vortices, neglected in Eq. (A8), generate ± 2 charged green and white vortices, and hybrid green-white ones. The corresponding fugacities turn out to be irrelevant variables in range of couplings we are interested in, so we can neglect these effects.

To implement the renormalization procedure, we want to carry out explicitly only the integrals over $\vec{x}$, $\vec{y}$, $\vec{X}$, and $\vec{Y}$, and leave the remaining integrations intact. Separating out the parts of $\bar{H}_{M,N}$ which depend on $\vec{r}_k$ and $\vec{r}_l$, or $\vec{R}_s$ and $\vec{R}_t$, we must consider

$$I_{kl}=\int d^2\vec{x}\int^{\delta} d^2\vec{y}\exp\left[2\pi K_a\sum_{\substack{i=1\\ i\neq k,l}}^{M}m(\vec{r}_i)[G(\vec{r}_i-\vec{r}_k)-G(\vec{r}_i-\vec{r}_l)]\right]\exp\left[2iq\sum_{j=1}^{N}n(\vec{R}_j)[\tilde{G}(\vec{R}_j-\vec{r}_k)-\tilde{G}(\vec{R}_j-\vec{r}_l)]\right] , \quad \text{(A13)}$$

and

$$I_{st}=\int d^2\vec{X}\int^{\delta} d^2\vec{Y}\exp\left[2\pi K_b\sum_{\substack{j=1\\ j\neq s,t}}^{N}n(\vec{R}_j)[G(\vec{R}_j-\vec{R}_s)-G(\vec{r}_j-\vec{R}_t)]\right]\exp\left[2iq\sum_{i=1}^{M}m(\vec{r}_i)[\tilde{G}(\vec{r}_i-\vec{R}_s)-\tilde{G}(\vec{r}_i-\vec{R}_t)]\right] , \quad \text{(A14)}$$

In writing Eqs. (A13) and (A14), we have set $m(\vec{r}_k) = -m(\vec{r}_l) = +1$, and $n(\vec{R}_s) = -n(\vec{R}_t) = 1$. These expressions simplify upon using Eqs. (A9) – (A12) to eliminate $\vec{r}_k$, $\vec{r}_l$, $\vec{R}_s$, and $\vec{R}_t$, and then expanding in y and Y

$$G(\vec{r}_j - \vec{r}_k) - G(\vec{r}_i - \vec{r}_l) \simeq (\vec{y}\cdot\vec{\nabla}_x) G(\vec{r}_i - \vec{x}) \ , \tag{A15}$$

$$\tilde{G}(\vec{R}_j - \vec{r}_k) - \tilde{G}(\vec{R}_j - \vec{r}_l) \simeq (\vec{y}\cdot\vec{\nabla}_x) \tilde{G}(\vec{R}_j - \vec{x}) \ , \tag{A16}$$

$$G(\vec{R}_j - \vec{R}_s) - G(\vec{R}_j - \vec{R}_t) \simeq (\vec{Y}\cdot\vec{\nabla}_X) G(\vec{R}_j - \vec{X}) \ , \tag{A17}$$

$$\tilde{G}(\vec{r}_i - \vec{R}_s) - \tilde{G}(\vec{r}_i - \vec{R}_t) \simeq (\vec{Y}\cdot\vec{\nabla}_X) \tilde{G}(\vec{r}_i - \vec{X}) \ . \tag{A18}$$

Upon expanding the exponentials to second order in $\vec{y}$ and $\vec{Y}$, and averaging over orientations of these variable, we can eliminate $\tilde{G}$ in favor of G by exploiting the identity

$$(\vec{\nabla} G)^2 = (\vec{\nabla}\tilde{G})^2 \ . \tag{A19}$$

An integration by parts then allows us to use the relation

$$\nabla^2 G(\vec{r}) = 2\pi\delta(\vec{r}) \tag{A20}$$

to eliminate the integrations over $\vec{x}$ and $\vec{X}$. After manipulations of this kind, and taking the limit of small δ, we find results which are independent of k, l, s, and t, namely,

$$I_{kl} = 2\pi\delta a \left[A - 2\pi^3 K_a^2 a^2 \sum_{\vec{r}\neq\vec{r}'} m(\vec{r}) m(\vec{r}') G(\vec{r} - \vec{r}') + \tfrac{1}{2}\pi q^2 a^2 \sum_{\vec{r}\neq\vec{r}'} n(\vec{r}) n(\vec{r}') G(\vec{r} - \vec{r}') \right] , \tag{A21}$$

$$I_{st} = 2\pi\delta a \left[A - 2\pi^3 K_b^2 a^2 \sum_{\vec{r}\neq\vec{r}'} n(\vec{r}) n(\vec{r}') G(\vec{r} - \vec{r}') + \tfrac{1}{2}\pi q^2 a^2 \sum_{\vec{r}\neq\vec{r}'} m(\vec{r}) m(\vec{r}') G(\vec{r} - \vec{r}') \right] , \tag{A22}$$

where A is the area of the system. The summations are over pairs of the remaining $(M-2)$ green and $(N-2)$ white vortices.

Inserting Eqs. (A21) and (A22) into Eqs. (A8) and (A5b), we see that terms proportional to the area renormalize the charge-independent part of $\bar{H}$. Since there are now two fewer vortices, the remaining terms in Eqs. (A21) and (A22) give $O(y_z^2)$ and $O(y_b^2)$ renormalizations of the logarithmic interaction in $\bar{H}$. Proceeding exactly as in the Appendix of the paper by Kosterlitz,[24] we can rescale y_a and y_b to produce a Hamiltonian of the same form as Eq. (A1). Upon iterating this procedure until the effective core diameter is increased from a to ae^l, we find renormalized couplings $K_a(l)$, $y_a(l)$, $K_b(l)$, and $y_b(l)$ which are solutions of

$$\frac{dK_a}{dl} = -4\pi^3 K_a^2 y_a^2 + \pi q^2 y_b^2 \ , \tag{A23}$$

$$\frac{dy_a}{dl} = (2 - \pi K_a) y_a \ , \tag{A24}$$

$$\frac{dK_b}{dl} = -4\pi^3 K_b^2 y_b^2 + \pi q^2 y_a^2 \ , \tag{A25}$$

$$\frac{dy_b}{dl} = (2 - \pi K_b) y_b \ . \tag{A26}$$

As a check on these results, we set $K_a = q^2/4\pi^2 K_b \equiv K$ initially, and find that this self-duality condition is preserved under our renormalization transformation

$$\frac{d}{dl}\left[K_a(l) - \frac{q^2}{4\pi^2 K_b(l)} \right] = 0 \tag{A27}$$

as it should be. Indeed, in this limit we recover the results of José *et al.*[20] Recursion relations for this special self-dual problem have also been derived using the Kosterlitz method by Elitzur *et al.*[32] Upon setting $q = 1$, K_6/p^2, $y_b = y_6$, $K_b = K_h$, and $y_b = y_h$, we find the results (2.62) quoted in the text.

Recursion formulas for the Hamiltonian (2.46a) appropriate near A in Fig. 4 can be found in the same way provided we make the replacement

$$iq\tilde{G}(\vec{r} - \vec{r}') \to \frac{2\pi g}{p} G(\vec{r} - \vec{r}') \tag{A28}$$

in Eq. (A1), and in subsequent equations. Since there is now a logarithmic interaction between green and white vortices, one expects that configurations of, say (+) green and (−) white pairs will be favored in addition to (±) green and (±) white pairings. These new complexions generate hybrid vortex-disclinations like the one shown in Fig. 7. It is easily checked

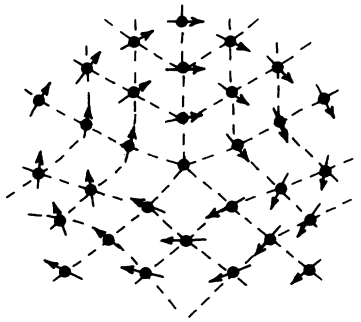

FIG. 7. Hybrid "vortex disclination" on a square lattice. Excitations of this kind are shown to be irrelevant in the text.

however, that the fugacity of such hybrids has the eigenvalue

$$\lambda_{\text{hybrid}} = 2 - \pi K_a - \pi K_b \ , \tag{A29}$$

which is negative (irrelevant) for $K_a \gtrsim 2/\pi$. Ignoring these irrelevant hybrids, and setting $q = -i\pi g/p$, $K_a = K_6/p^2$, $y_a = y_6$, $K_b = K_1$, and $y_b = y_1$, we recover the recursion relations (2.47) quoted in Sec. II C.

APPENDIX B: EVALUATION OF $C_\times(\vec{r})$

We now evaluate the cross-correlation function $C_\times(r)$, defined in Sec. II B, in the unlocked phase C^*. For this purpose we may ignore vortices and disclinations; however, we cannot set $h = 0$, even though h is formally an "irrelevant variable." As we shall see, $C_\times(r)$ is itself of order h. To first order in h, we have

$$\begin{aligned} C_\times(r) &= \langle \exp[6i\theta(\vec{r})] \exp[-6i\phi(\vec{0})] \\ &\quad \times \exp\left(h \int d^2r' \cos[6\theta_-(\vec{r}')]\right)\rangle_{h=0} \\ &\approx h \int d^2r' \langle \exp[6i\theta(\vec{r})] \exp[-6i\phi(\vec{0})] \\ &\quad \times \cos[6\theta(\vec{r}')]\rangle_{h=0} \ , \end{aligned} \tag{B1}$$

where the expectation values on the right-hand side of Eq. (B1) are taken with $h = 0$, as indicated. After expressing θ and ϕ in terms of the variables θ_+ and θ_-, defined in Sec. II B, we find

$$\begin{aligned} C_\times(\vec{r}) &= h \langle \exp\{6i[\theta_+(\vec{r}) - \theta_+(\vec{0})]\}\rangle_{h=0} \\ &\quad \times \int d^2r' \langle \exp\{6i[\alpha\theta_-(\vec{0}) + \beta\theta_-(\vec{r}) \\ &\quad - \theta_-(\vec{r}')]\}\rangle_{h=0} \ . \end{aligned} \tag{B2}$$

The expectation values may be evaluated using Eq. (2.41) with $h \equiv 0$. Making use of the relation $\alpha + \beta = 1$, which implies that

$$\begin{aligned} &[\alpha\theta_-(\vec{0}) + \beta\theta_-(\vec{r}) - \theta_-(\vec{r}')]^2 \\ &\quad = \alpha[\theta_-(\vec{r}') - \theta_-(\vec{0})]^2 + \beta[\theta_-(\vec{r}') - \theta_-(\vec{r})]^2 \\ &\quad - \alpha\beta[\theta_-(\vec{r}) - \theta_-(\vec{0})]^2 \ , \end{aligned} \tag{B3}$$

we find

$$C_\times(r) = h\left(\frac{1}{r}\right)^{\eta_+ - \alpha\beta\eta_\Delta} \int d^2r' \left(\frac{1}{r'}\right)^{\alpha\eta_\Delta} \left(\frac{1}{|\vec{r} - \vec{r}'|}\right)^{\beta\eta_\Delta} \ , \tag{B4}$$

where $\eta_+ = 18/\pi K_+$ and η_Δ is given by Eq. (1.11).

In the C^* phase, we necessarily have $\eta_\Delta > 4$, so that the integral (B4) is convergent at large distances. If the gradient-coupling constant g is not too large, then the inequalities (1.13) and (1.14) imply that $\beta\eta_\Delta < 2$ and hence $\alpha\eta_\Delta > 2$. Thus, the integral is formally divergent at $\vec{r}' = \vec{0}$, and the major contribution to the integral comes from the region where r' is close to the short-distance cutoff.

We therefore find

$$C_\times(r) = (\text{const})\, h r^{-\eta_\times} \ , \tag{B5}$$

where

$$\eta_\times = \eta_+ + \beta(1 - \alpha)\eta_\Delta = \eta_6 \ . \tag{B6}$$

The value of the constant in Eq. (B5) depends on the nature of the short-distance cutoff, and of course, this will be modified if we include the effects of dislocations and vortices. However, the dependence on r is correct, for sufficiently large r, provided we use the renormalized value of η_6.

In principle, if g is large, there can be a region of the C^* phase where $\beta > \alpha$, or equivalently a region where $\eta_6 > 36\eta_1$. In this case, the integral (B4) will be dominated by the region $|\vec{r}' - \vec{r}| \simeq 0$, and the exponent $\eta_\times$ will be equal to $36\eta_1$. It should be noted, however, that the analysis used here to calculate the cross-correlation function $C_\times(r)$ will also lead to a term in $C_6(r)$ proportional to $h^2(1/r)^{36\eta_1}$. This term will actually dominate at large distances if we have $\eta_6 > 36\eta_1$. In this case, the leading terms in the long-distance behavior of the correlation function would have the same form as in the *locked* tilted phase C, and the C^* phase would be distinguished only by the behavior of corrections to the leading power law.

In the limit $r \to 0$, the correlation function $C_\times(r)$ becomes the expectation value $\langle \Delta(\vec{0}) \rangle$, where Δ is defined by Eq. (1.9). Clearly $\langle \Delta \rangle$ is nonzero, and is proportional to h for small h, in the C^* phase. The constant term in Eq. (1.10), for the large distance behavior of $C_\Delta(\vec{r})$ is of course equal to $|\langle \Delta \rangle|^2$. The second term in Eq. (1.10) can be obtained by the methods of Sec. II B, with $h = 0$ for convenience.

[1] J. M. Kosterlitz and D. J. Thouless, J. Phys. C 6, 1181 (1973).

[2] See also, V. L. Berezinskii, Zh. Eksp. Teor. Fiz. 59, 907 (1970) [Sov. Phys. JETP 32, 493 (1971)].

[3] See, e.g., W. Shockley, in *L'Etat Solide*, Proceedings of the Neuvieme Couseil de Physique, edited by R. Stoops (Institut International de Physique Solvay, Brussels, 1952).

[4] D. R. Nelson, Phys. Rev. B 18, 2318 (1978).

[5]B. I. Halperin and D. R. Nelson, Phys. Rev. Lett. 41, 121 (1978); 41, 519(E) (1978); D. R. Nelson and B. I. Halperin, Phys. Rev. B 19, 2457 (1979).

[6]A. P. Young, Phys. Rev. B 19, 1855 (1979).

[7]D. Frenkel and J. P. McTague, Phys. Rev. Lett. 42, 1632 (1979).

[8]R. M. J. Cotterill and L. B. Pedersen, Solid State Commun. 10, 439 (1972).

[9]R. Morf, Phys. Rev. Lett. 43, 931 (1979); see also, D. J. Thouless, J. Phys. C 11, L189 (1978).

[10]C. C. Grimes and G. Adams, Phys. Rev. Lett. 42, 795 (1979).

[11]C. Y. Young, R. Pindak, N. A. Clark, and R. B. Meyer, Phys. Rev. Lett. 40, 773 (1978).

[12]C. Rosenblatt, R. Pindak, N. A. Clark, and R. B. Meyer, Phys. Rev. Lett. 42, 1220 (1979).

[13]R. J. Birgeneau and J. D. Litster, J. Phys. Lett. (Paris) 39, L399 (1978).

[14]D. E. Moncton and R. Pindak, Phys. Rev. Lett. 43, 70 (1979).

[15]P. Pershan, G. Aeppli, R. Birgeneau, and J. Litster (private communication); see also, J. D. Litster, R. J. Birgeneau, M. Kaplan, C. R. Safinya, and J. Als-Nielsen, Lecture notes for NATO Advanced Study Institute, Geilo, Norway, 1979 (Plenum, New York, to be published).

[16]The quantities K_1, K_6, and g are ordinary stiffness constants divided by $k_B T$; thus, they are dimensionless. On a microscopic level, the constants K_1, K_6, and g are actually *tensors* with different eigenvalues referring to gradients parallel to and perpendicular to the local tilt orientation. We ignore this complication in the present paper. In any case, the tensors become isotropic in the limit of very long wavelengths. See Refs. 11, 12, and 21 and D. R. Nelson and R. Pelcovits, Phys. Rev. B 16, 2191 (1977).

[17]It is intriguing to speculate that the C_1 and C_2 phases, if they exist as distinct phases in two dimensions, may have three-dimensional analogs in bulk smectic-C and smectic-F liquid crystals. See. Ref. 18. We are grateful to R. Pindak for bringing the smectic-F phase to our attention.

[18]For x-ray-diffraction studies of smectic-H, -F, and -C phases, see A. J. Leadbetter, J. P. Gaughan, B. Kelley, G. W. Gray, and J. Goodby, J. Phys. (Paris) 40, C3-178 (1979). See also J. J. Benattar, J. Doucet, M. Lambert, and A. M. Levelut (unpublished).

[19]See Ref. 5 and N. D. Mermin, Phys. Rev. 176, 250 (1968).

[20]J. José, L. P. Kadanoff, S. Kirkpatrick, and D. R. Nelson, Phys. Rev. B 16 1217 (1977).

[21]D. R. Nelson and J. M. Kosterlitz, Phys. Rev. Lett. 39, 1201 (1977).

[22]R. A. Pelcovits and B. I. Halperin, Phys. Rev. B 19, 4614 (1979).

[23]See D. Stein, Phys. Rev. B 18, 2397 (1978).

[24]J. M. Kosterlitz, J. Phys. C 7, 1046 (1974).

[25]L. P. Kadanoff, J. Phys. C 11, 1399 (1978).

[26]A. Luther and I. Peschel, Phys. Rev. B 9, 2911 (1974).

[27]S. Coleman, Phys. Rev. D 11, 2088 (1972).

[28]P. W. Anderson and G. Yuval, J. Phys. C 4, 607 (1971).

[29]See, e.g., Appendix A of A. N. Berker and D. R. Nelson, Phys. Rev. B 19, (1979), as well as Appendix B of the second part of Ref. 5.

[30]A. A. Migdal, Zh. Eksp. Teor. Fiz. 69, 810 (1975) [Sov. Phys. JETP 42, 413 (1976)]; Zh. Eksp. Teor. Fiz. 69, 1457 (1975) [Sov. Phys. JETP 43, 743 (1976)].

[31]L. P. Kadanoff, Ann. Phys. (N.Y.) 100, 359 (1976).

[32]S. Elitzur, R. Pearson, and J. Shigemitzu, Phys. Rev. D 19, 3698 (1979).